

## Electron capture and $\alpha$ -particle decay of $^{190}\text{Pb}$

Y. A. Ellis-Akovali and K. S. Toth

*Oak Ridge National Laboratory, Oak Ridge, Tennessee 37830*

C. R. Bingham

*University of Tennessee, Knoxville, Tennessee 37916 and Oak Ridge National Laboratory, Oak Ridge, Tennessee 37830*

H. K. Carter

*UNISOR, Oak Ridge, Tennessee 37830*

D. C. Sousa

*Eastern Kentucky University, Richmond, Kentucky 40475*

(Received 12 August 1980)

We are investigating the decay properties of even-even lead nuclei with  $A \leq 192$  in an effort to understand their anomalous  $\alpha$ -decay rates as reported by Hornshøj *et al.* Our results for  $^{192}\text{Pb}$  were recently published. In this study  $^{190}\text{Pb}$ ,  $T_{1/2} = 1.2 \pm 0.1$  min, was produced in the  $^{180}\text{W}(^{16}\text{O}, 6n)$  reaction and its decay was investigated with the use of an on-line isotope separator facility. Singles and coincidence  $\gamma$ -ray and conversion-electron data were accumulated. In addition, singles  $\gamma$ -ray and  $\alpha$ -particle spectra were taken with the detectors positioned in calibrated geometries. Twenty-three transitions were identified and placed into a scheme incorporating 16 levels in  $^{190}\text{Tl}$ . With this decay scheme information and the absolute photon and  $\alpha$ -particle intensities, the  $^{190}\text{Pb}$   $\alpha$ -decay branch was determined to be  $(9.0 \pm 2.0) \times 10^{-3}$ , a value about four times greater than that reported by Hornshøj *et al.* Our new results for  $^{190}\text{Pb}$  and  $^{192}\text{Pb}$  indicate that the lead  $\alpha$ -decay reduced widths may show a dependence on neutron number observed for other elements.

[RADIOACTIVITY  $^{190}\text{Pb}$  measured  $T_{1/2}$ ,  $E_\gamma$ ,  $I_\gamma$ ,  $I_{ce}$ ,  $E_\alpha$ ,  $I_\alpha$ ,  $\gamma\gamma$ ,  $ce\gamma$  coin;  $^{190}\text{Tl}$  deduced levels;  $^{190}\text{Pb}$  deduced  $\alpha$ -decay reduced width. Mass separation.]

### I. INTRODUCTION

Hornshøj *et al.*<sup>1</sup> have reported that the  $\alpha$ -decay reduced widths of  $^{186}$ ,  $^{188}$ ,  $^{190}$ ,  $^{192}\text{Pb}$  behave in an unusual manner. In contrast to the expectation that these widths should decrease as one approaches the  $N=126$  closed shell, they were instead found to increase by about a factor of 30 between  $^{186}\text{Pb}$  ( $N=104$ ) and  $^{192}\text{Pb}$  ( $N=110$ ).

In Ref. 1 the electron-capture plus positron ( $\text{EC}+\beta^+$ ) decay strengths were determined from  $K$  x-ray intensities. Such determinations are subject to a number of corrections. A more precise method involves using a known ( $\text{EC}+\beta^+$ ) decay scheme. To this end we undertook the investigation of the ( $\text{EC}+\beta^+$ ) decay properties of these proton-rich lead isotopes with the use of the Oak Ridge on-line isotope separator facility. Our main purpose was to determine more accurate values for the  $\alpha$  branches of  $^{186}$ ,  $^{188}$ ,  $^{190}$ ,  $^{192}\text{Pb}$ . The  $^{192}\text{Pb}$  study was completed recently.<sup>2</sup> Herein we present and discuss the  $^{190}\text{Pb}$  data.

A target of  $^{180}\text{W}$  (isotopic enrichment of 92.6%) was bombarded with  $^{16}\text{O}$  ions to produce  $^{190}\text{Pb}$  in the  $^{180}\text{W}(^{16}\text{O}, 6n)$  reaction. Following mass separation an automated tape system was used to collect  $A=190$  nuclides and to transport them to the counting stations. Singles and coincidence  $\gamma$ -ray and conversion-electron data were taken.

The coincidence information was accumulated in a three-word list mode, either  $\gamma$ - $\gamma$ - $\tau$  or  $e$ - $\gamma$ - $\tau$ ; the singles measurements were made in a multi-spectrum mode so that half-life information could be obtained. In separate experiments, singles  $\gamma$ -ray and  $\alpha$ -particle spectra were measured simultaneously with the two detectors placed in known geometries so that their absolute efficiencies could be determined with standard calibration sources.

### II. DECAY OF $^{190}\text{Pb}$ TO $^{190}\text{Tl}$

Figures 1 and 2 show the  $\gamma$ -ray spectrum accumulated during the first 70 sec of counting which followed 635 collection cycles, each 180 sec in duration. The spectrum, up to about 2 MeV, is shown in Fig. 1; Fig. 2 shows only the low-energy portion of the spectrum, expanded to display more detail. The conversion-electron spectrum taken during the same time is shown in Fig. 3. For half-life information the 180-sec counting interval in these measurements was divided into 10-sec bins. Transitions were then assigned to  $^{190}\text{Pb}$  decay on the basis of the nuclide's half-life of  $1.2 \pm 0.1$  min as well as the observation of coincidences with thallium  $K$  x rays. In Figs. 1-3  $^{190}\text{Pb}$  transitions are labeled by energy; most of the remaining peaks belong to the

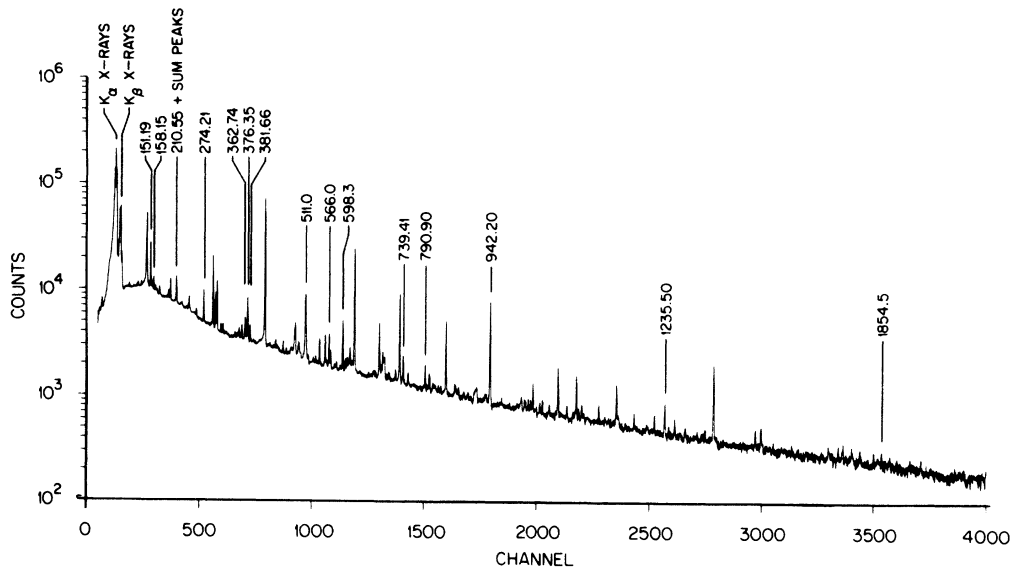


FIG. 1. Gamma-ray spectrum measured for  $A = 190$  accumulated during the first 70 sec after the end of 635 production and collection cycles, each 180 sec in duration. Only peaks assigned to the decay of  $^{190}\text{Pb}$  are labeled with energy.

decay of  $^{190}\text{Tl}$ ,  $^{190}\text{Hg}$  (Ref. 3), and  $^{190}\text{Au}$  (Ref. 4). Table I lists the  $^{190}\text{Pb}$  transition energies, photon intensities, and deduced multipolarities. The  $\gamma$ - $\gamma$  and  $e$ - $\gamma$  coincidence results are summarized in Table II.

The  $^{190}\text{Pb}$  ( $\text{EC} + \beta^+$ ) decay scheme, based on the information given in Tables I and II, is shown in Fig. 4. Numbers following  $\gamma$ -ray energies and multipolarities in the figure represent total tran-

sition intensities. They were calculated from our photon intensities and from theoretical conversion coefficients.<sup>5,6</sup> Multipolarities were deduced from photon and electron intensities, normalized so that the 731.1- and 416.4-keV transitions in  $^{190}\text{Hg}$  and the 295.8-keV transition in  $^{190}\text{Pt}$  came out to be pure  $E2$  in character (see Refs. 3 and 4, respectively).

High- and low-spin isomers are known<sup>3</sup> to exist

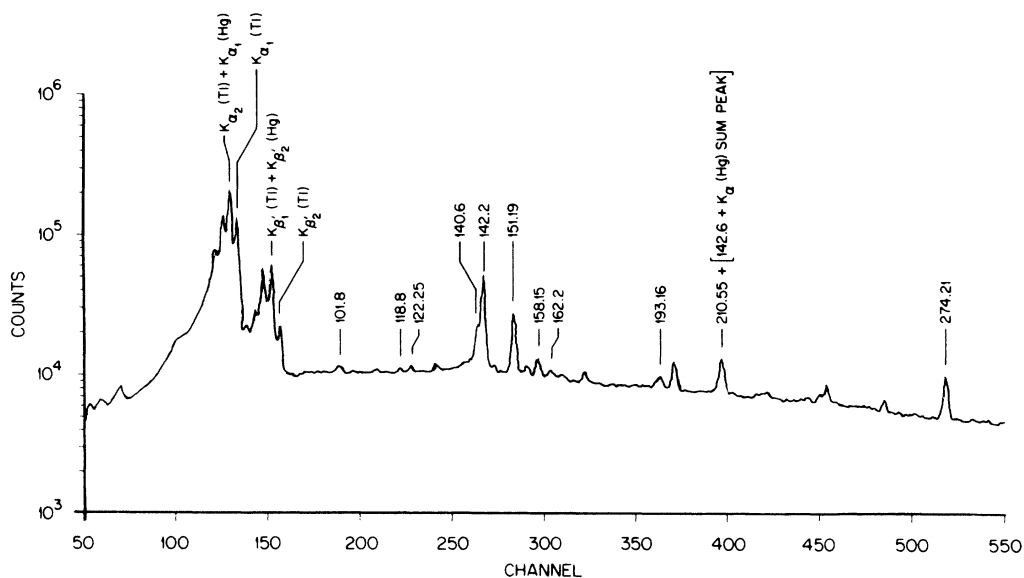


FIG. 2. Low-energy portion of the  $\gamma$ -ray spectrum displayed in Fig. 1, expanded to show more detail. Peaks labeled with energy are assigned to  $^{190}\text{Pb}$  decay.

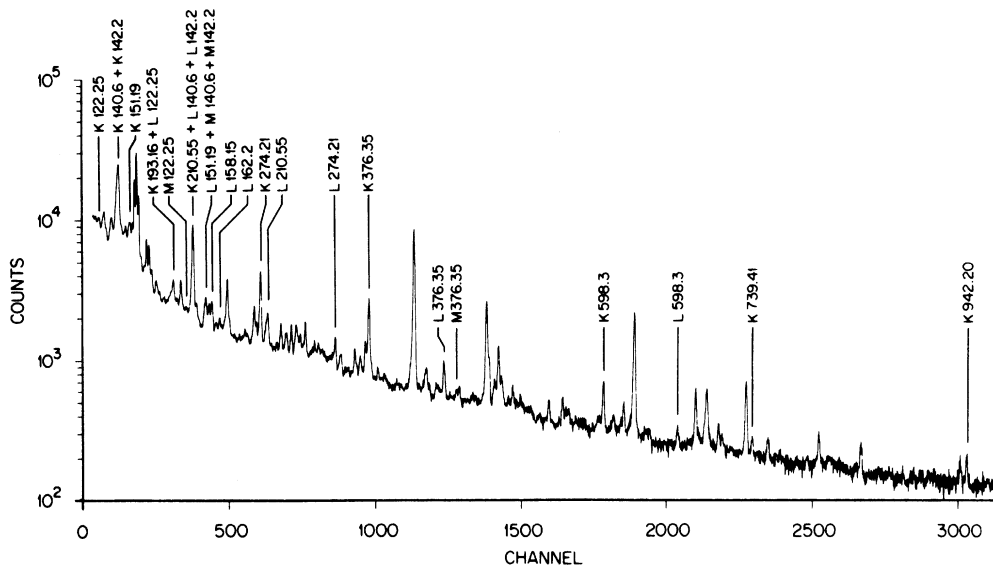


FIG. 3. Conversion-electron spectrum measured for  $A = 190$  accumulated during the first 70 sec after the end of 635 production and collection cycles, each 180 sec in duration. Peaks labeled by energy are assigned to transitions following the decay of  $^{190}\text{Pb}$ .

in  $^{190}\text{Tl}$ , but their relative excitations have not been determined. The systematics of these isomeric states in odd-odd thallium nuclei will be

discussed below. For now, we will note that it is extremely unlikely that the high-spin state is involved in the decay of the  $^{190}\text{Pb}$  ground state. If,

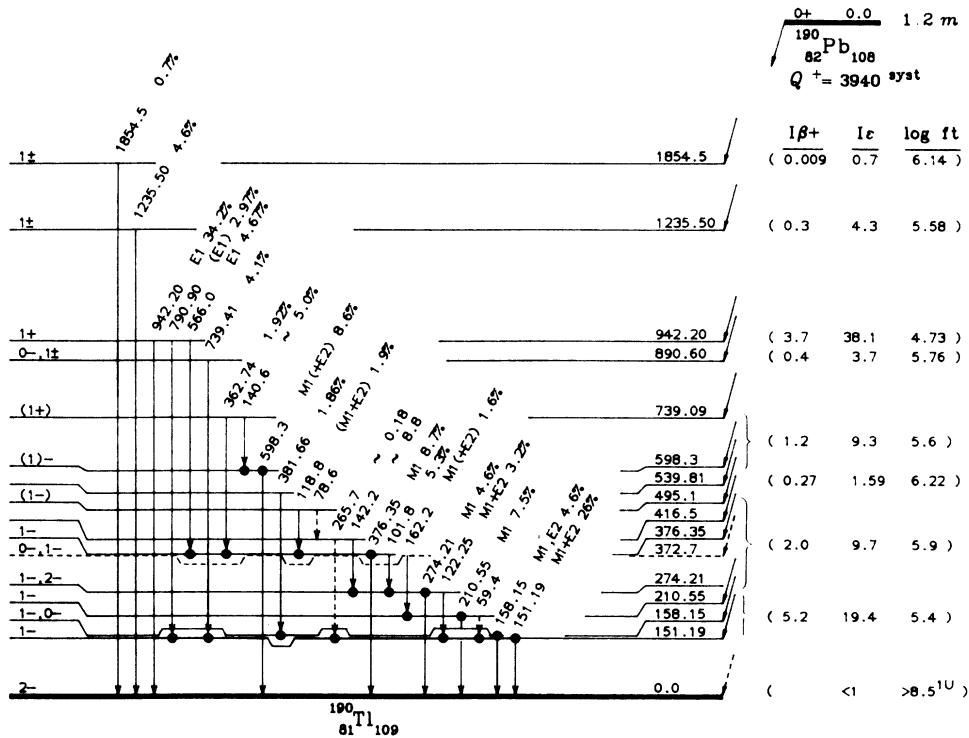


FIG. 4. The  $^{190}\text{Pb}$  decay scheme. Dots indicate observed coincidences. Numbers following transition energies and multipolarities represent total intensities per 100  $^{190}\text{Pb}$  electron-capture plus positron decays. If the  $2^-$  state in  $^{190}\text{Tl}$ , which is indicated as being the ground state, is in fact an isomeric level, then the excitation energies of all the  $^{190}\text{Tl}$  levels would have to be raised.

TABLE I. Energies, photon intensities, and multiplicities of transitions in  $^{190}\text{Tl}$ .

$E_\gamma$ (keV)	$I_\gamma^a$	Multipolarity
K x ray	1030 <sup>b</sup> (130)	
59.4 <sup>c</sup>		
78.6 <sup>c</sup>		
101.8 (2)	7.3 (10)	
118.8 (2)	4.1 (10)	(M1 + E2)
122.25 (20)	7.4 (9)	M1 + E2
140.6 (3)	130 (50)	
142.2 (3)		
151.19 (10)	100 (2)	M1 + E2
158.15 (15)	19.1 (17)	M1, E2
162.2 (2)	5.5 (19)	M1 (+E2)
193.16 <sup>d</sup> (15)	14.5 (20)	
210.55 (13)	40 (10)	M1
265.7 <sup>e</sup> (3)	~1.9	
274.21 (10)	34 (6)	M1
362.74 (15)	21 (3)	
376.35 (10)	79 (10)	M1
381.66 (15)	20.4 (20)	E1
566.0 (2)	51.7 (26)	
598.3 (2)	90 (7)	M1 (+E2)
739.41 (15)	46 (5)	
790.90 (20)	33 (3)	(E1)
942.20 (10)	380 (30)	E1
1235.50 (15)	51 (5)	
1854.5 (3)	7.7 (20)	

<sup>a</sup>Relative intensities based on a value of 100 for the 151.19-keV transition. For absolute intensities per 100 electron-capture decays, relative intensities should be multiplied by a factor of 0.090 (8).

<sup>b</sup>The calculated intensity of K x rays expected from K-electron conversions and K captures is 1070 (125).

<sup>c</sup>Obscured in  $\gamma$  and electron singles; observed only in coincidence spectra.

<sup>d</sup>Transition is not placed in the decay scheme.

<sup>e</sup>Assignment to  $^{190}\text{Pb}$  decay is not definite.

however, the low-spin state in  $^{190}\text{Tl}$  is the isomer, then the level energies indicated in Fig. 4 would have to be shifted upward by the isomeric-state energy. Based on the decay pattern<sup>3</sup> of the low-spin  $^{190}\text{Tl}$  state, its spin has to be 2 or greater. In that case the most favorable  $\beta$  decay would involve a first-forbidden unique transition,  $0^+ - 2^-$ . According to the rules adopted by the Nuclear Data Project, the  $\log ft$  value for such a beta transition must be  $> 8.5$ , which in turn means that the direct decay to the  $^{190}\text{Tl}$  low-spin isomer must be  $< 1\%$ . On this basis then, the sum of the total intensities of the  $\gamma$ -ray transitions terminating at this level was assumed to represent 100% of all  $^{190}\text{Pb}$  (EC +  $\beta^*$ ) decays. Direct decay strengths, indicated in Fig. 4., to the various excited states were deduced from the intensity balance at each level. Then, with an estimated<sup>7</sup> EC decay energy of 3.94 MeV, the  $\log ft$  values were calculated. These are also shown in Fig. 4.

The  $\log ft$  value of 4.7 calculated for the electron-capture branch feeding the 942.2-keV level means that this  $\beta$  transition is allowed; the parity of the 942.2-keV level, therefore, must be positive. The E1 multipolarity of the 942.2-keV  $\gamma$  transition then determines the spin and parity of the base and 942.2-keV levels to be  $2^-$  and  $1^+$ , respectively. For the remaining levels shown in Fig. 4, spins and parities were deduced on the basis of these two assignments, multiplicities, and  $\log ft$  values.

By considering available single-particle orbitals, Bingham *et al.*<sup>3</sup> noted that  $7^+$  was the probable assignment for the  $^{190}\text{Tl}$  high-spin isomer. They suggested a  $(\pi s_{1/2} \nu_{13/2}^i)_{7^+}$  configuration for this level based on the strength of its decay to a pos-

TABLE II. Summary of  $\gamma$ - $\gamma$  and  $e$ - $\gamma$  coincidence results.

Gates (keV)	Coincident transitions (keV)
K x rays (Tl)	K x rays, all $\gamma$ 's listed in Table I
151.19	K x rays, (59.4), 101.8, 122.25, 140.6, 142.2, 162.2, 265.7, annihilation radiation, 739.41, 790.90
158.15	K x rays, 381.66
210.55	K x rays, 162.2
274.21	K x rays, (78.6), 101.8, 142.2, 362.74, annihilation radiation, 566.0
376.35	K x rays, 118.8, 362.74, 566.0
381.66	K x rays, 158.15
511.00 <sup>a</sup>	K x rays, 151.19, 162.2, 193.16, 265.7, 274.21, 566.0, 598.3, 739.41, 790.90, 942.20, 1235.50
566.0	K x rays, 274.21, 376.35, annihilation radiation
598.3	K x rays, 140.6, annihilation radiation
739.41	K x rays, 151.19, annihilation radiation
790.90	K x rays, 151.19, annihilation radiation
942.20	K x rays, annihilation radiation

<sup>a</sup>Annihilation radiation.

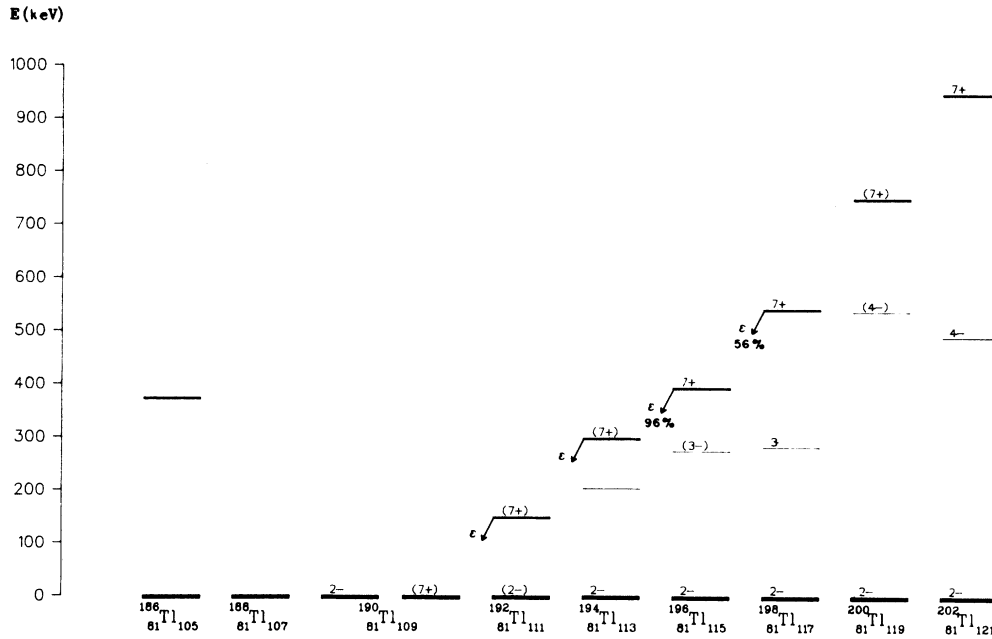


FIG. 5. Systematics of the  $7^+$  and  $2^-$  isomeric states in odd-odd thallium nuclei.

sible two-quasiparticle  $(\nu i_{13/2} \nu p_{3/2})_{5^-}$  state in  $^{190}\text{Hg}$ . The existence of  $2^-$  and  $7^+$  isomeric levels in  $^{190}\text{Tl}$  is consistent with the systematic observation (see Fig. 5) of these two states in doubly-odd thallium nuclei. From measured spins and magnetic moments (see, e.g., data compiled in Ref. 8) the main configurations for these states in  $^{194-204}\text{Tl}$  are  $(\pi s_{1/2} \nu f_{5/2})_{2^-}$  and  $(\pi s_{1/2} \nu i_{13/2})_{7^+}$ . The  $2^-$  states are the ground states for those isotopes. As the neutron number decreases, however, the  $7^+$  level drops in energy, and the relative position of the  $2^-$  and  $7^+$  states in  $^{192}\text{Tl}$  and beyond has not been experimentally determined.

Although the systematics might also imply a  $(\pi s_{1/2} \nu f_{5/2})$  configuration for the  $2^-$  state in  $^{190}\text{Tl}$ , an examination of states in  $N=109$  isotones and in odd- $A$  thallium nuclei reveals other possible combinations of proton and neutron states coupling to  $2^-$ . The  $\frac{1}{2}[510]$  neutron orbital originating from the  $f_{5/2}$  shell state was assigned for the ground states of light, prolately deformed  $N=109$  isotones, e.g.,  $^{181}\text{Hf}$ ,  $^{183}\text{W}$ , and  $^{185}\text{Os}$ . For those nuclei, the  $\frac{3}{2}[512]$  orbital originating from the  $p_{3/2}$  shell state is an excited state, and its energy decreases with increasing mass number. In fact, the  $\frac{3}{2}$  level is the ground state for  $^{187}\text{Pt}$ .  $^{189}\text{Hg}$  is considered<sup>9</sup> to be oblately deformed, and the  $\frac{3}{2}[532]$  orbital was assigned to one of its isomeric levels. Whether or not this level is the ground state is yet undetermined. The other isomer has the spin of  $\frac{1}{2}^+$ , presumably because of the  $i_{13/2}$

orbital. Therefore, in addition to the  $f_{5/2}$  state, the  $\frac{3}{2}^-$  and  $\frac{1}{2}^+$  neutron states are also possible.

Similarly, the intruder  $h_{9/2}$  proton state is known to decrease in energy as one approaches  $^{189}\text{Tl}$  from both  $^{201}\text{Tl}$  and  $^{185}\text{Tl}$ . Therefore, the  $2^-$  state in  $^{190}\text{Tl}$  could be  $(\pi s_{1/2} \nu p_{3/2})$  or  $(\pi h_{9/2} \nu i_{13/2})$ , as well as  $(\pi s_{1/2} \nu f_{5/2})$ . Because of the large uncertainties involved for the electron-capture feedings to various levels in  $^{190}\text{Hg}$  from the  $2^-$  isomer, the structure of this level cannot at this time be positively stated.

We examined our singles and coincidence data for possible isomeric transitions in  $^{190}\text{Tl}$ . None was observed. We also calculated the  $K$  x-ray intensity due to  $K$  captures to observed levels in  $^{190}\text{Tl}$  and  $K$  conversions of all electromagnetic transitions by using the computer programs developed by the Nuclear Data Project. The calculated value agrees well with our experimental intensity (see Table I for the comparison). In addition, decay-curve analyses of the  $K_{\alpha_1}$  and  $K'_{\beta_2}$  x-ray peaks showed a 1.2-min half-life with no indication of a longer-lived component due to  $^{190}\text{Tl}$  isomeric decay. These observations suggest that if isomeric transitions exist, they are either weak or their energies are below the thallium  $K$  binding energy.

### III. THE $\alpha$ -DECAY RATE OF $^{190}\text{Pb}$

The  $^{190}\text{Pb}$   $\alpha$ -decay branching ratio was determined in experiments where the efficiencies for

the  $\gamma$ -ray and  $\alpha$  particle detectors had been absolutely calibrated. The  $(\text{EC}+\beta^+)$  strength was calculated from the intensities of the 151.2- and 942.2-keV  $\gamma$  rays using the decay scheme information presented above. The  $\alpha$ -decay strength was calculated from the intensity of the single  $\alpha$  group known<sup>1</sup> to belong to  $^{190}\text{Pb}$ . The ratio of the two strengths yielded an  $\alpha$  branch of  $(9.0 \pm 2.0) \times 10^{-3}$ .

In discussing  $\alpha$ -decay rates, it is customary to consider them within a theoretical framework in which relative probabilities can be obtained after removing the dependence on  $Q$  value and on the atomic and mass numbers. As in Ref. 2, we will use the formalism developed by Rasmussen.<sup>10</sup> In it a reduced width  $\delta^2$ , is defined by the equation  $\lambda = \delta^2 P/h$ , where  $\lambda$  is the decay constant,  $h$  is Planck's constant, and  $P$  is the penetrability factor calculated for the  $\alpha$  particle to tunnel through a barrier. This barrier includes an optical model potential derived from the analysis<sup>11</sup> of low-energy  $\alpha$ -particle scattering data. A centrifugal barrier is also added so that  $l$  dependence in  $\alpha$  decay can be taken into account.

Three quantities are needed to deduce an  $\alpha$ -decay reduced width, i.e., decay energy, half-life, and an  $\alpha$ /total branching ratio. In Table III we compare our  $^{190}\text{Pb}$  data with those presented in Ref. 1. While differences can be noted between the two sets of energies and half-lives, the largest discrepancy involves the branching ratios, our value being about four times greater. The new value of the  $\alpha$  branch raises the reduced width from 0.021 to 0.094 MeV (see Table III). It is this result, together with our recently determined<sup>2</sup>  $^{192}\text{Pb}$   $\alpha$  width, that we wish to discuss within the context of  $\alpha$ -decay rates in the lead region.

Figure 6 shows reduced widths for doubly-even neutron-deficient nuclei with  $Z$  from 78 to 88 plotted as a function of  $N$ . Most of the experimental information used to calculate the reduced widths is taken from a recent compilation.<sup>12</sup> Only transitions between the ground states of these nuclei are included in the figure. These

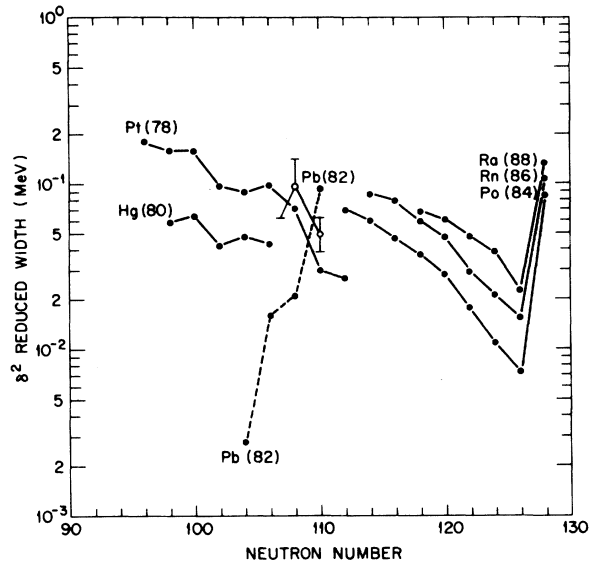


FIG. 6. Reduced widths for  $s$ -wave  $\alpha$  transitions plotted versus neutron number for proton-rich isotopes with  $Z$  from 78 to 88. The open points for  $^{190}\text{Pb}$  and  $^{192}\text{Pb}$  are the result of our investigations (present study and Ref. 2), while the closed points (connected by the dashed line) for  $\text{Pb}(82)$  are deduced from data in Ref. 1.

$s$ -wave transitions are considered to represent unhindered decays, and their widths are used to determine hindrance factors for other types of  $\alpha$  transitions. A rather regular behavior as a function of both neutron and atomic number is observed for  $s$ -wave  $\alpha$  decays. Their reduced widths are largest for nuclei two or four particles beyond a closed shell (with sharp minima occurring at the closed shell) followed by a decrease as one approaches the next closure. Less pronounced minima have been observed for subshell closures, such as the one at  $Z = 64$  (see Ref. 13). One sees in Fig. 6 that, with the exception of the lead isotopes, the trends do manifest themselves. The reduced widths decrease both as  $N = 126$  and  $Z = 82$  are approached. Fluctuations in the case of platinum and mercury isotopes are a reflection of the difficulties involved in studying short-lived nuclei far from stability. However, the basic patterns with  $N$  and  $Z$  exist for both elements.

The dashed line in Fig. 6 connects the  $^{186,188,190,192}\text{Pb}$  widths calculated from the data presented in Ref. 1. This behavior of  $\delta^2$  with respect to neutron number is contrary to the normal trend. The open points for  $^{190}\text{Pb}$  and  $^{192}\text{Pb}$  are the result of our current investigations. As noted above, the new value for  $^{190}\text{Pb}$  is about a factor of 4 larger because of the increase in the  $\alpha$  branch

TABLE III.  $\alpha$ -decay properties of  $^{190}\text{Pb}$ .

	Present study	Ref. 1
$E_\alpha$ (keV)	5577 $\pm$ 5	5590
$T_{1/2}$ (min)	1.2 $\pm$ 0.1	1.1
$\alpha$ /total	$(9.0 \pm 2.0) \times 10^{-3}$	$2.1 \times 10^{-3}$
$\delta^2$ (MeV)	0.094 $^{+0.036}_{-0.028}$	0.021

from  $2.1 \times 10^{-3}$  to  $9.0 \times 10^{-3}$ . The open  $^{192}\text{Pb}$  point is down by a factor of 2, primarily because of the fact that we measured<sup>2</sup> the nuclide's half-life to be 3.5 min, rather than 2.2 min as presented in Ref. 1. (This half-life was reported in the  $\alpha$ -decay study of Le Beyec *et al.*,<sup>14</sup> where the counting statistics appear to be poor.) The line joining the two newly determined  $^{190,192}\text{Pb}$  reduced widths indicates that the lead isotopes may very well follow the general dependence with  $N$  observed for other elements. To see if this is indeed so, the study should be extended to include  $^{188}\text{Pb}$  and  $^{186}\text{Pb}$ . In particular, one should note that the  $^{186}\text{Pb}$  width (Ref. 1) is based, not on a measured  $\alpha$  branch, but rather on an estimate from anticipated cross section for the production of this isotope in heavy-ion-induced reactions.

## ACKNOWLEDGMENTS

The authors would like to thank M. A. Ijaz and J. Lin for their help in some of the data-taking phases of this investigation and W. B. Ewbank for assistance with computer programs and graphics. Oak Ridge National Laboratory is operated by Union Carbide Corporation for the U. S. Department of Energy under Contract No. W-7405-eng-26. UNISOR is a consortium of 13 institutions and is partially supported by them and by the U. S. Department of Energy under Contract No. DE-AC05-76OR00033 with Oak Ridge Associated Universities. Nuclear physics research at the University of Tennessee is supported by the U. S. Department of Energy under Contract No. DE-AS05-76ER04936.

<sup>1</sup>P. Hornshøj, P. G. Hansen, B. Jonson, H. L. Ravn, L. Westgaard, and O. B. Nielsen, Nucl. Phys. A230, 365 (1974).

<sup>2</sup>K. S. Toth, M. A. Ijaz, C. R. Bingham, L. L. Riedinger, H. K. Carter, and D. C. Sousa, Phys. Rev. C 19, 2399 (1979).

<sup>3</sup>C. R. Bingham *et al.*, Phys. Rev. C 14, 1586 (1976).

<sup>4</sup>A. Johansson and B. Nyman, Phys. Scr. 8, 99 (1973).

<sup>5</sup>R. S. Hager and E. C. Seltzer, Nucl. Data, Sec. A 4, 1 (1968).

<sup>6</sup>O. Dragoun, Z. Plajner, and F. Schmutzler, Nucl. Data Tables A9, 119 (1971).

<sup>7</sup>A. H. Wapstra and K. Bos, At. Data Nucl. Data Tables

19, 175 (1977).

<sup>8</sup>*Table of Isotopes*, seventh ed., edited by C. M. Lederer and V. S. Shirley (Wiley, New York, 1978).

<sup>9</sup>J. Bonn, G. Huber, H.-J. Kluge, and E. W. Otten, Z. Phys. A 276, 203 (1976).

<sup>10</sup>J. O. Rasmussen, Phys. Rev. 113, 1593 (1959).

<sup>11</sup>G. Igo, Phys. Rev. Lett. 1, 72 (1958).

<sup>12</sup>H. Gauvin, Y. Le Beyec, J. Livet, and J. L. Reyss, Ann. Phys. (Paris) 9, 241 (1975).

<sup>13</sup>W.-D. Schmidt-Ott and K. S. Toth, Phys. Rev. C 13, 2574 (1976).

<sup>14</sup>Y. Le Beyec, M. Lefort, J. Livet, N. T. Porile, and A. Siivola, Phys. Rev. C 9, 1091 (1974).